Effect of ambient on the resistance fluctuations of graphene

Kazi Rafsanjani Amin and Aveek Bid[a)]
Department of Physics, Indian Institute of Science, Bangalore 560 012, India

(Received 2 April 2015; accepted 24 April 2015; published online 5 May 2015)

In this letter, we present the results of systematic experimental investigations of the effect of different chemical environments on the low frequency resistance fluctuations of single layer graphene field effect transistors. The shape of the power spectral density of noise was found to be determined by the energetics of the adsorption-desorption of molecules from the graphene surface making it the dominant source of noise in these devices. We also demonstrate a method of quantitatively determining the adsorption energies of chemicals on graphene surface based on noise measurements. We find that the magnitude of noise is extremely sensitive to the nature and amount of the chemical species present. We propose that a chemical sensor based on the measurement of low frequency resistance fluctuations of single layer graphene field effect transistor devices will have extremely high sensitivity, very high specificity, high fidelity, and fast response times. © *2015 AIP Publishing LLC*. [http://dx.doi.org/10.1063/1.4919793]

The study of low frequency $1/f$ noise in graphene monolayer is interesting from both scientific as well as technological points of view. The specific surface area (2630 m^2/g) of single layer graphene (SLG) is amongst the highest in layered materials making the conductance of graphene extremely sensitive to the ambient—the presence of a few foreign molecules on its surface can significantly modify its electrical noise characteristics. The low defect levels of pristine graphene[1–5] ensure that intrinsic flicker noise due to thermal switching of defects is lower than any semiconductor material.[6–10] These distinctly unique properties of single layer graphene make it exceptionally suited for use as chemical or radiation sensors.

Resistance fluctuation of pristine SLG field effect transistor (SLG-FET) devices under high vacuum conditions has been studied in detail.[4–8] There is considerable debate in the community as to which of the two possible mechanisms is the dominant cause of noise in pristine SLG-FET devices[6]—(1) mobility fluctuations due to charged scattering centers on substrate and device surface or (2) number density fluctuations due to charged impurities on surface of device or on the substrate. Although the effect of various chemical gas molecules on the resistance of the SLG-FET devices has been studied,[11–13] there is very little study of the effect of exposure to different chemicals on the resistance fluctuations of SLG-FET devices. There has been a previous study of the effect of adsorbed molecules on resistance fluctuation spectrum,[14] but a quantitative study of the energetics of the processes giving rise to the resistance fluctuations is missing.

SLG-FET devices were fabricated on SiO_2 substrates by mechanical exfoliation from natural graphite followed by conventional electron beam lithography process.[1] A false color scanning electron microscope (SEM) image of a typical device is shown in Figure 1(a). The SLG is shown in violet, while the yellow strips are the electrical contact lines made by thermally evaporating 5 nm of Cr and 70 nm of Au.

The devices were tested after the lithography process for the presence of resist residues using Atomic Force Microscope (AFM) and Raman spectroscopy. A typical image of AFM scan and Raman spectrum is shown in Figures 1(b) and 1(c), respectively. The surface roughness of the device is estimated from the AFM line scans (~0.55 nm), and the absence of a D peak and the position of the G peak (1582.2 cm^{-1}) in Raman spectra indicate negligibly small extrinsic doping.[16–19] Quantum Hall measurements[1] and Raman spectroscopy[17] on representative devices were used to confirm that the graphene flakes were monolayers. The resistance of the devices was measured by standard low frequency ac techniques using a lock-in amplifier in a 4 probe configuration. A plot of the sheet resistance $R_\square$ as a function of the back-gate voltage V_g with the device in vacuum is shown in Figure 1(d). The room temperature mobility of the devices was extracted from these measurements using the method described in Ref. 15. The mobility values lay in the range $10\,000 - 26\,000\ cm^2\ V^{-1}\ s^{-1}$ attesting to the high quality of the devices.[20]

The power spectral density (PSD) of voltage fluctuations $S_V(f)$ across the SLG-FET devices was measured as a function of frequency f over a bandwidth of 1 Hz to 1 kHz using an ac auto-correlation method [for details of the noise measurement and analysis process, see Ref. 21]. A typical PSD of pristine SLG-FET device measured at 295 K is shown in Figure 2. The red open circles are the measured background noise, while the black solid line is the expected thermal noise for the device at 295 K. The excellent match between the two curves shows that the background noise arises primarily due to thermal noise of the device and that extraneous instrumentation noise was negligible. The olive filled circles are the measured resistance fluctuation noise from the device (after subtracting out the background noise). It was seen that the PSD of pristine SLG-FET devices was always $1/f$ in nature. For these (and all subsequent) measurements, the chemical potential of the device was positioned where the response of the sheet resistance $R_\square$ to the V_g was maximum (marked by the red dots in Figure 1(d)).

[a)]Electronic mail: aveek.bid@physics.iisc.ernet.in. URL: http://www.physics.iisc.ernet.in/~aveek_bid/aveek.html

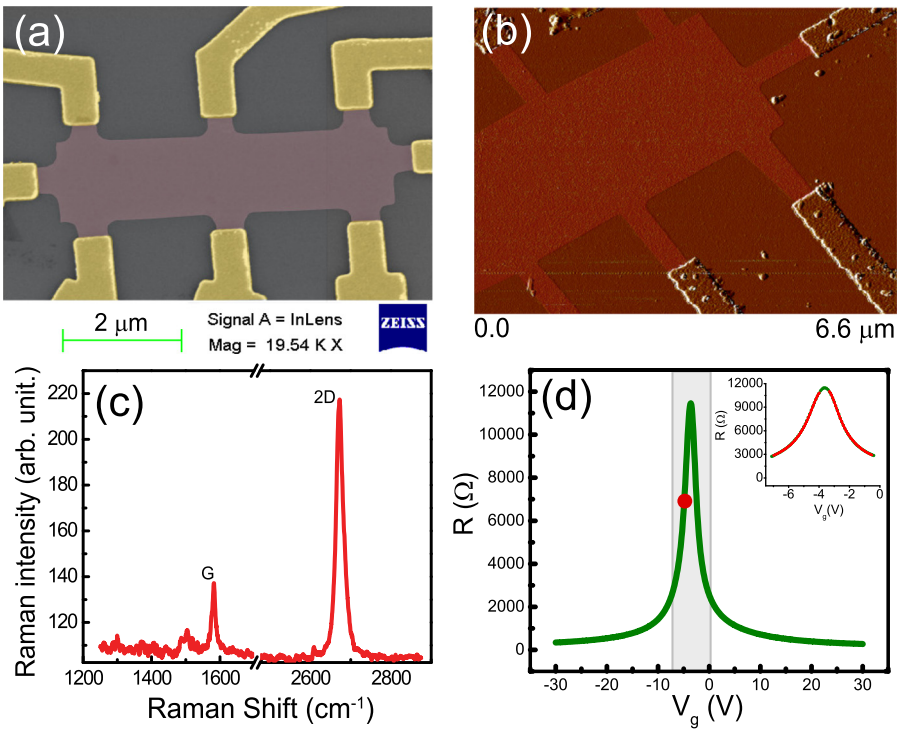

FIG. 1. False color (a) SEM image and (b) AFM image of typical SLG-FET devices showing the cleanliness of the surface after the fabrication process. The surface roughness on the graphene extracted from AFM scan was 0.549 nm. (c) Raman spectrum of the SLG-FET device after lithography process. (d) Sheet resistance $R_{\square}$ of the device as a function of back gate voltage V_g. The mobility of the device extracted from the data was $20\,000\,\mathrm{cm^2V^{-1}s^{-1}}$. Inset: Plot of $R - V_g$ data (shown in green circles) over a narrow range of V_g. The red lines are the fit to the data using equation mentioned in Ref. 15. The fitting region is marked by gray box in the main plot.

To quantify the effect of different chemical environments on the resistance fluctuations of SLG-FET devices, we compare the PSD of the voltage fluctuations in the presence of different chemical species. An example is shown in Figure 3(a) where we plot the frequency dependence of the PSD of voltage fluctuations measured when the SLG-FET device is exposed to chloroform and methanol in two separate runs. For comparison, we also show the normalized PSD of the pristine device. [Note that we have plotted the quantity $f \times S_V(f)/V^2$ for $1/f$ noise; the plot would be parallel to the frequency axis.] We find that the PSD shows Lorentzian humps at characteristic frequencies which allows us to fingerprint different chemicals. The data from these measurements

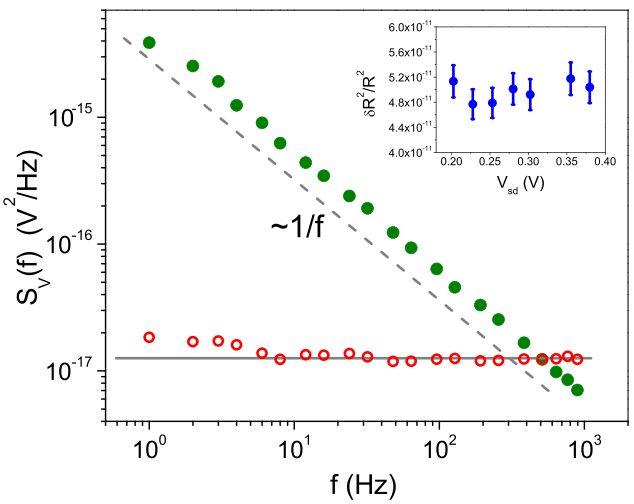

FIG. 2. A typical 1/f noise spectrum (olive filled circles) and background thermal noise (red open circles) of a pristine graphene monolayer FET device. The black solid line shows the expected background noise, while the grey dotted line shows a reference 1/f curve. The inset shows the $\delta R^2/R^2$ as a function of V_{sd}.

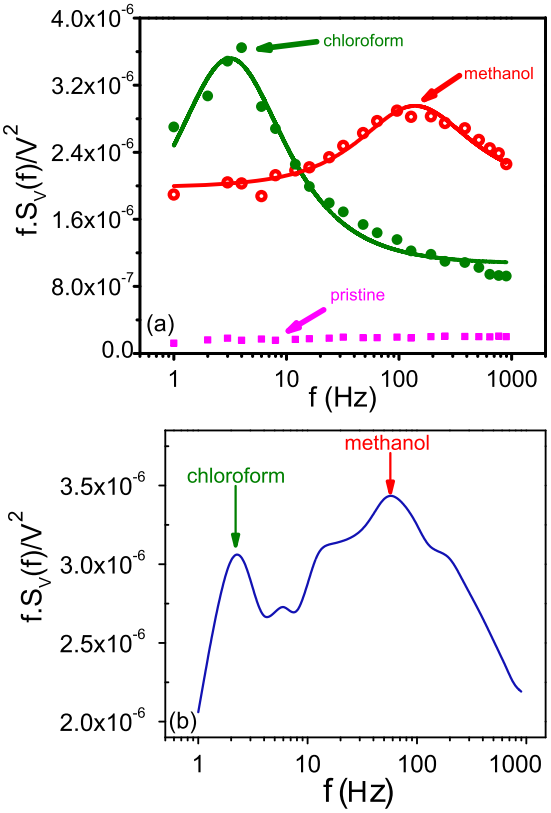

FIG. 3. (a) Plot of scaled PSD as a function of frequency measured under different conditions—for the pristine device kept in vacuum (pink filled square), after exposure to 100 ppm methanol (red open circle) and after exposure to 100 ppm chloroform (olive filled circle). The solid lines are the fits to the experimental data using Eq. (1). (b) Plot of scaled PSD measured after the device was exposed to a mixture of 100 ppm methanol and 100 ppm chloroform—the characteristic frequencies of both methanol and chloroform are marked by arrows.

were analyzed using an empirical relation that consisted of a $1/f$ term and a Lorentzian with a characteristic component[22]

$$S_V(f) = \frac{A}{f} + \frac{Bf_C}{f^2 + (f_C)^2}, \quad (1)$$

where A and B are constants are extracted from fits to the experimental data. The solid lines in Figure 3(a) are the fits to the experimental data using Eq. (1). The magnitude of the non $1/f$ noise component (quantified by the parameter B) contains information about the amounts of the chemical species the device has been exposed to while the shape of the PSD (parametrized by the Lorentzian of corner frequency f_C) acts as unique spectroscopic fingerprints that helps to identify the chemical. An example of this is given in Figure 3(b) where we plot the response of the device when it was exposed to a mixture of 100 ppm chloroform and 100 ppm methanol—the spectrum clearly shows the presence of both the chemical species. Such unique determination of analytes is obviously not possible in a detection scheme based on the measurement on resistance changes alone. The parameters B/A and f_C for 100 ppm of different chemical analytes extracted from our measurements are presented in Table I—the values of f_C match very well with the earlier reports.[14]

The relative variance of the resistance fluctuations $\delta R^2/R^2$ (which we refer to as noise) was obtained by integrating the PSD $S_R(f)$ over the bandwidth of measurement

$$\frac{\delta R^2}{R^2} = \frac{\int_{f_{min}}^{f_{max}} f S_R(f) df}{R^2}. \quad (2)$$

Figure 4 shows the plot of the percentage changes in R and $\delta R^2/R^2$ measured simultaneously in a typical measurement where the device was exposed to 100 ppm of nitrobenzene vapor. For the initial 15 min, the device was kept in vacuum and both the R and $\delta R^2/R^2$ measured to establish the base values. As soon as nitrobenzene was introduced (at the instant of time marked by grey line), both R and $\delta R^2/R^2$ started increasing with time and eventually saturated. The change in R was about 50%, whereas the change in $\delta R^2/R^2$ is 1000%, more than an order of magnitude higher. The chamber evacuation was then started at the time shown in the figure as grey dotted line and both R and $\delta R^2/R^2$ started decreasing towards the baseline values. The resistance of the device took more than an hour to regain its initial value. This large response time of the resistance change in graphene devices exposed to a chemical environment has been seen before[23–25] and is one of the major bottlenecks in implementing chemical sensors based on SLG-FET. The noise of the device on the other hand resets to the baseline value within a few seconds of starting the chamber evacuation. We have performed similar measurements for different chemicals like acetone, methanol, chloroform, and ammonia, and with eight different devices. The response of R and $\delta R^2/R^2$ of the SLG-FET in all these cases was qualitatively similar with the exact response depending on the type and amount of the chemical. From these measurements, we can conclude that there are at least two major differences between the response of resistance and resistance fluctuations of graphene devices to change in the chemical environment—(1) the magnitude of relative change in noise is much larger and (2) the typical time scale associated with changes in noise is much smaller.

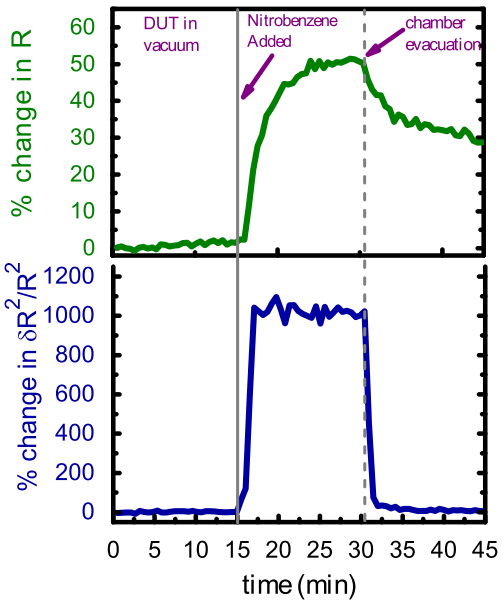

FIG. 4. Plot of change in R (top panel, olive line) and change in $\delta R^2/R^2$ (bottom panel, blue line) with time for a typical measurement with the SLG-FET device exposed to 100 ppm of nitrobenzene.

The drastically different trends of change in R and in $\delta R^2/R^2$ upon exposure to a chemical environment can be understood from the following simple picture. The average resistance R and resistance fluctuations $\delta R^2/R^2$ in a sample arise from quite distinct mechanisms. Static scatterers can have an appreciable effect on the resistance of a device while having negligible effect on its resistance fluctuations. On the other hand, the presence of dynamic scatterers even with a weak scattering potential can have a large affect on the resistance fluctuation spectrum while having very little effect on the average resistance.[26] Changes in the resistance of a graphene device due to change in ambient conditions are directly related to the amount of the analyte molecules adsorbed on its surface. The resistance of the device can go back to the baseline value only after desorption of all the adsorbed molecules from the surface. This process is very slow for graphene and might take up to few hours, depending upon the quantity and type of molecule adsorbed.[23,24]

Resistance fluctuations, on the other hand, arise primarily due to fluctuations in both the number density and mobility of the charge carriers in the system.[6] For a semiconductor device exposed to a chemical environment, there are three primary sources of resistance fluctuations: dynamic adsorption-desorption of the chemical species from the device surface,

TABLE I. Values of the parameters f_C and B/A for different chemical species.

Chemical species	f_C	B/A
Methanol	138.68	0.977
Nitrobenzene	82.0895	1.7582
Chloroform	3.156	4.571
Ammonia	9.659	0.3942

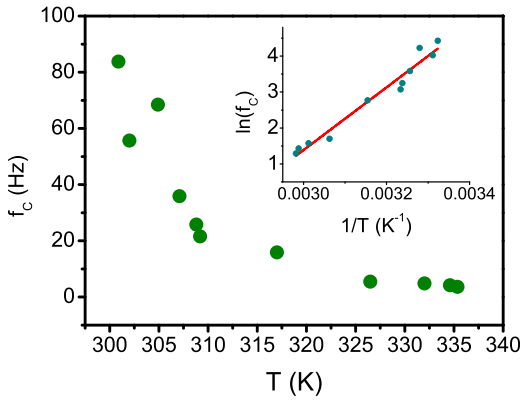

FIG. 5. Plot of f_C as a function of temperature over the range of 300 K to 340 K. (inset) The filled circles show the plot of logarithm of f_C as a function of inverse temperature; the red line is the fit to the data using Eq. (3).

dynamic percolative motion of the chemical species on the device surface, and charge trapping-detrapping by the chemical species.[27–30] It was predicted that amongst these three possible mechanisms, adsorption-desorption noise caused by fluctuations of the equilibrium number of adsorbed molecules in the device should dominate the resistance fluctuations seen in metallic sensors[28,29] The adsorption-desorption process giving rise to the resistance fluctuations in the device is facilitated by the presence of a reservoir of analyte vapours close to the graphene surface. Pumping out the analyte vapours depletes this reservoir rapidly. This slows down the adsorption-desorption process and this slow desorption continues till all the analytes have been removed from the device. A detailed analysis is presented in the supplementary material.[20]

If adsorption-desorption noise is really the dominant source of resistance fluctuations in SLG-FET exposed to a chemical environment, then f_C should be related to the adsorption-desorption energy E_a of the specific gas molecule on SLG-FET through the equation[22,26]

$$f_C = f_0 \exp\left(\frac{-E_a(T)}{k_B T}\right), \tag{3}$$

where f_0 is the attempt frequency for the thermally activated process.

To test this hypothesis, we have measured the temperature dependence of noise in SLG-FET devices in the presence of chemical vapors over the temperature range of 300 K–340 K. In Figure 5, we show a plot of f_C as a function of temperature extracted from these measurements—the data presented here have been obtained by exposing the SLG-FET device to 200 ppm of methanol. The inset shows a plot of the logarithm of f_C as a function of inverse temperature; the red line is a least-square linear fit to Eq. (3). The linearity of the data shows that the activation energy is temperature independent as expected over this narrow temperature range. The value of E_a extracted from the slope of the curve is 752.3 meV ± 6.30%, which matches well the calculated values of adsorption energy of methanol on SLG-FET.[31]

To conclude, we have studied the effect of different chemical environments on the resistance fluctuations of single layer graphene FET devices. Our measurements indicate that the main source of noise in these devices is number density fluctuation arising from adsorption-desorption process of the chemicals at the graphene surface. We also find that a detection scheme based on the measurement of resistance fluctuations is far superior to the traditional method of measuring the average resistance change in terms of sensitivity, specificity, and the response time of the detector.

The work was supported by NPMASS, Aeronautical Development Agency (ADA), Government of India. The authors acknowledge device fabrication and characterization facilities in CeNSE, IISc, Bangalore. K.R.A. thanks CSIR, MHRDG, India, for financial support and Phanindra Sai for help and useful discussions on lithography.

[1]K. S. Novoselov, A. K. Geim, S. V. Morozov, D. Jiang, Y. Zhang, S. V. Dubonos, I. V. Grigorieva, and A. A. Firsov, "Electric field effect in atomically thin carbon films," Science **306**, 666–669 (2004).
[2]Y.-M. Lin and P. Avouris, "Strong suppression of electrical noise in bilayer graphene nanodevices," Nano Lett. **8**, 2119–2125 (2008).
[3]K. R. Ratinac, W. Yang, S. P. Ringer, and F. Braet, "Toward ubiquitous environmental gas sensors–capitalizing on the promise of graphene," Environ. Sci. Technol. **44**, 1167–1176 (2010).
[4]Q. Shao, G. Liu, D. Teweldebrhan, A. A. Balandin, S. Rumyantsev, M. Shur, and D. Yan, "Flicker noise in bilayer graphene transistors," IEEE Electron Device Lett. **30**, 288–290 (2009).
[5]A. N. Pal, V. Kochat, and A. Ghosh, "Direct observation of valley hybridization and universal symmetry of graphene with mesoscopic conductance fluctuations," Phys. Rev. Lett. **109**, 196601 (2012).
[6]A. A. Balandin, "Low-frequency 1/f noise in graphene devices," Nature Nanotechnol. **8**, 549–555 (2013).
[7]G. Xu, C. M. Torres, Jr., Y. Zhang, F. Liu, E. B. Song, M. Wang, Y. Zhou, C. Zeng, and K. L. Wang, "Effect of spatial charge inhomogeneity on 1/f noise behavior in graphene," Nano Lett. **10**, 3312–3317 (2010).
[8]A. N. Pal, S. Ghatak, V. Kochat, E. Sneha, A. Sampathkumar, S. Raghavan, and A. Ghosh, "Microscopic mechanism of 1/f noise in graphene: Role of energy band dispersion," ACS Nano **5**, 2075–2081 (2011).
[9]A. Kaverzin, A. S. Mayorov, A. Shytov, and D. Horsell, "Impurities as a source of 1/f noise in graphene," Phys. Rev. B **85**, 075435 (2012).
[10]B. Pellegrini, "1/f noise in graphene," Eur. Phys. J. B **86**, 373 (2013).
[11]K. R. Amin and A. Bid, "Graphene as a sensor," Curr. Sci. **107**, 430–436 (2014).
[12]W. Yuan and G. Shi, "Graphene-based gas sensors," J. Mater. Chem. A **1**, 10078–10091 (2013).
[13]F. Yavari and N. Koratkar, "Graphene-based chemical sensors," J. Phys. Chem. Lett. **3**, 1746–1753 (2012).
[14]S. Rumyantsev, G. Liu, M. S. Shur, R. A. Potyrailo, and A. A. Balandin, "Selective gas sensing with a single pristine graphene transistor," Nano Lett. **12**, 2294–2298 (2012).
[15]W. Zhu, V. Perebeinos, M. Freitag, and P. Avouris, "Carrier scattering, mobilities, and electrostatic potential in monolayer, bilayer, and trilayer graphene," Phys. Rev. B **80**, 235402 (2009).
[16]L. M. Malard, M. A. Pimenta, G. Dresselhaus, and M. S. Dresselhaus, "Raman spectroscopy in graphene," Phys. Rep. **473**, 51 (2009).
[17]A. C. Ferrari, J. C. Meyer, V. Scardaci, C. Casiraghi, M. Lazzeri, F. Mauri, S. Piscanec, D. Jiang, K. S. Novoselov, S. Roth, and A. K. Geim, "Raman spectrum of graphene and graphene layers," Phys. Rev. Lett. **97**, 187401 (2006).
[18]A. Das, S. Pisana, B. Chakraborty, S. Piscanec, S. Saha, U. Waghmare, K. Novoselov, H. Krishnamurthy, A. Geim, A. Ferrari, and A. K. Sood, "Monitoring dopants by Raman scattering in an electrochemically top-gated graphene transistor," Nat. Nanotechnol. **3**, 210–215 (2008).
[19]A. C. Ferrari, "Raman spectroscopy of graphene and graphite: Disorder, electron–phonon coupling, doping and nonadiabatic effects," Solid State Commun. **143**, 47–57 (2007).
[20]See supplementary material at http://dx.doi.org/10.1063/1.4919793 for details of mobility calculation and for the analysis of the time scales associated with changes in resistance and noise.
[21]J. H. Scofield, "Ac method for measuring low-frequency resistance fluctuation spectra," Rev. Sci. Instrum. **58**, 985–993 (1987).

[22]A. Bid, A. Guha, and A. K. Raychaudhuri, "Low-frequency random telegraphic noise and 1/*f* noise in the rare-earth manganite $pr_{0.63}ca_{0.37}mno_3$ near the charge-ordering transition," Phys. Rev. B **67**, 174415 (2003).
[23]F. Schedin, A. Geim, S. Morozov, E. Hill, P. Blake, M. Katsnelson, and K. Novoselov, "Detection of individual gas molecules adsorbed on graphene," Nat. Mater. **6**, 652–655 (2007).
[24]G. Chen, T. M. Paronyan, and A. R. Harutyunyan, "Sub-ppt gas detection with pristine graphene," Appl. Phys. Lett. **101**, 053119 (2012).
[25]S. Rumyantsev, G. Liu, R. Potyrailo, A. Balandin, and M. Shur, "Selective sensing of individual gases using graphene devices," IEEE Sens. J. **13**, 2818–2822 (2013).
[26]M. B. Weissman, "$\frac{1}{f}$ noise and other slow, nonexponential kinetics in condensed matter," Rev. Mod. Phys. **60**, 537–571 (1988).
[27]I. Jokić, Z. Djurić, M. Frantlović, K. Radulović, P. Krstajić, and Z. Jokić, "Fluctuations of the number of adsorbed molecules in biosensors due to stochastic adsorption–desorption processes coupled with mass transfer," Sens. Actuators, B **166**, 535–543 (2012).
[28]J. G. Sami Gomri, J.-L. Seguin, and K. Aguir, "A mobility and free carriers density fluctuations based model of adsorption–desorption noise in gas sensor," J. Phys. D: Appl. Phys. **41**, 065501 (2008).
[29]L. Kish, R. Vajtai, and C. Granqvist, "Extracting information from noise spectra of chemical sensors: Single sensor electronic noses and tongues," Sens. Actuators, B **71**, 55–59 (2000).
[30]J. Ederth, J. Smulko, L. Kish, P. Heszler, and C. Granqvist, "Comparison of classical and fluctuation-enhanced gas sensing with pdxwo3 nanoparticle films," Sens. Actuators, B **113**, 310 (2006).
[31]T. Pankewitz and W. Klopper, "*Ab initio* modeling of methanol interaction with single-walled carbon nanotubes," J. Phys. Chem. C **111**, 18917 (2007).